Title

An investigation of low velocity impact properties of rotationally moulded skin-foam-skin sandwich structure

Abu Saifullah[a*1], Ben Thomas[a], Robert Cripps[b], Kamran Tabeshfar[a], Lei Wang[c]

[a] Bournemouth University, Talbot Campus, BH12 5BB, UK. E-mail: Thomasb@bmth.ac.uk, ktabeshf@bournemouth.ac.uk

[b] Longitude Consulting Engineers Ltd., UK. E-mail: b.cripps@longitude.uk.com

[c] Matrix Polymers, UK. E-mail: lei.wang@matrixpolymers.com

Corresponding Author-

[a*1] Abu Saifullah

Bournemouth University, Talbot Campus, BH12 5BB, UK.

E-mail: abu.saifullah@port.ac.uk
naserbiomaterials@gmail.com

Acknowledgements

We express our sincere thanks to Matrix Polymers, UK and Longitude Consulting Engineers Ltd. for the rotational moulding of skin-foam-skin sandwich structures and test samples development.

[1] School of Mechanical and Design Engineering, University of Portsmouth, Anglesea Road, Anglesea Building, Portsmouth, Hampshire PO1 3DJ, UK

Abstract

In this study, the low velocity impact properties of rotationally moulded skin-foam-skin sandwich structures were investigated experimentally since there is a need for a greater understanding of the impact behaviour of these composites in service to extend the range of their applications. Polyethylene rotationally moulded sandwich structures were manufactured at various skin and core layer thickness combinations and tested using an instrumented low velocity drop weight impact testing machine at 20J to 100J impact energy levels, at room temperature. This allowed the identification of the impact response, failure mode, the effects of the skin and core layer thickness on impact resistance. Force-deflection curves, maximum force, contact time, maximum deflection versus impact energy curves were analysed. Samples were seen to fail due to the indentation dart piercing the upper and lower skins, with crushing and consolidation seen in the core foamed layer. Delamination at the core/skin interface was not observed. It was found that fracture initiates from the lower skin and then continues to grow to the upper skin via the foamed core layer. The impact resistance was noted to increase with increasing skin and core layer thickness, though an increase in skin layer thickness had a greater contribution than an increase in the core layer thickness.

Keywords: Rotational moulding, skin-foam-skin, sandwich, low velocity impact, PE.

1. Introduction

Sandwich composite structures are made from a single material such as polyethylene (PE) using the rotational moulding process, have two solid skins separated by a foam core (Figure 1) [1, 2]. The main advantages of these sandwich structures are high specific stiffness and strength, good bending stiffness, lower weight, excellent thermal insulation and acoustic

damping when compared to a solid structure [1, 2]. The rotational moulding process provides excellent adhesion between the skin and core layers as these are made from the same material and form a seamless and continuous interface between the skin and foam layers [1- 3].

Rotational Moulding

Rotational moulding is an established and growing manufacturing method particularly suited to large hollow plastic parts, it consists of four stages (Figure 2)-

1. placing the polymer powder in the mould,
2. heating with application of biaxial rotation,
3. cooling to solidify the polymer melt into the desired shape
4. opening the mould and removal of the product [1, 2, 4-11].

Skin-foam-skin sandwich structures produced using rotational moulding generally involve laying down the skin and foam layers sequentially [3, 7, 12]. In the mould a standard skin powder, e.g. Polyethylene (PE) is added first, the mould is heated with rotation in the oven of the rotational moulding machine to melt and cover the interior of the mould with the first skin layer, the mould is then removed from the oven, opened and the powder for the foamed core layer is added before the mould is returned to the oven to create the foam layer. Once the foam layer is complete, the mould is again removed and opened to add the third (or inner) skin layer and placed it in the oven. For creating the foamed core layer, a controlled quantity of chemical foaming agent is mixed with the main polymer powder e.g. polyethylene powder [13-15]. This method has some disadvantages due to process interruptions as the mould needs to be opened for each additional layer. Therefore, a new method was patented in 1990 [16] where drop boxes are used to release the second and third layer powders. In this sophisticated process, the drop box is filled with foam-able powder. The main mould is charged with the skin material and

heated to melt the skin materials to coat the mould surface. When this step is complete, the drop box door is opened automatically and releases the second layer foam-able powder into the main mould. A foamed layer is produced in this way. Following this a second drop box is opened to form the inner skin layer. A key feature of manufacturing single material (the same PE material is used in skin and core layers) sandwich structures in this way is better interfacial adhesion between core and skin layers compared to traditional sandwich structure manufacturing processes where the skin and core layers are produced separately, then attached in a successive step [2].

The demand for rotationally moulded sandwich composites in small marine leisure craft and automotive applications are increasing with time, though the research work on the properties of these composite structures is limited. A. Boccaccio et al. [2] tested the edgewise compression behaviour, the relation between buckling response and core, skin thickness, as well as the effects of surface geometric imperfections for Polyethylene sandwich panels using both experimental and numerical analysis [2]. A thicker upper skin was found to create a larger deflection of the sandwich panel and the report concluded by recommending an increase in the thickness of the core layer to prevent buckling of the sandwich panel under load. Vazquez-Fletes et al. [7] characterised the Charpy and Gardner impact properties of three layered skin-foam-skin samples using linear medium density polyethylene (LMDPE) and agave fibre, LMDPE foam and LMDPE for the outer, core and inner layers respectively. Here, the effect of using agave fibre with LMDPE on impact properties was focused. Impact strength (Charpy and Gardner) was observed to decrease with agave fibre content because of poor interfacial adhesion between the matrix and agave fibres. Research was also conducted into the manufacturing parameters for single-charge rotational moulding of Polypropylene (PP) integral skin foam composite [3]. It was found that the heating profile, heating time and rate,

mould rotational speed, formulations and selection of resins or powders for skin and foam layers are important parameters for the manufacturing of integral skin-foam composites for avoiding any decomposition in the materials, immature activation of the foaming agent content, non-uniform skin thickness and unexpected skin and foamed core quality.

During the service life of rotationally moulded sandwich components (e.g. boat hulls, automotive applications etc.) impact damage by foreign objects are crucial. In small boat hull or automotive applications common impact events include collisions with floating debris, other crafts, docks, grounding, during production (e.g. tool drops), impacts between the fishing equipment and structure which are classified as low velocity impact damage [17]. Such damage may severely reduce the stiffness, stability and load carrying capacity of the structure as a whole [18-20]. According to Cantwell and Morton [21] less than 10 m/s impact velocity is considered for the low velocity impact whereas Abrate [18, 19] defined less than 100 m/s as a low velocity impact event. Low velocity impact is considered to be quasi-static as it generates an entire structural response, while high velocity impact creates localised damage as the structure does not get time to respond. Alongside the impact velocity, the ratio ($\bar{m}$) of the impact mass to the effective plate mass is important for low velocity impact as the impact response is considered quasi-static when the mass ratio is greater than eight ($\bar{m}$>8) [22]. Generally the impact response of sandwich composites such as fibre reinforced sandwich composites subjected to low velocity impact is influenced by the impactor dart diameter and geometry, impact velocity and mass, specimen thickness, and the thickness of skin and core layers. A larger contact force was found for the increased radius of the impactor, though less of this effect was observed for the displacement of the whole structure [23-25]. The impactor mass has a great influence on the impact event as it influences the structural response and impact duration to the applied impact force. A larger impact mass leads to longer impact

duration and larger deflection [22]. For small mass impacts, the impact response duration is very low and therefore it transfers a higher impact energy to the sandwich composite that causes earlier damage initiation and larger delamination compared to the large mass impact response. Skin and core layer thickness also play a crucial role in an impact event.

In addition to the above mentioned parameters, the strain rate is also considered one of the material characteristics that contributes to impact properties in high velocity impact [20]. The mechanical response of thermoplastic materials is affected by loading conditions such as strain rate and temperature [26]. Material temperature is influenced by its deformation as it is known that plastic work for deforming a material transforms partly into heat resulting in self-heating of the thermoplastic materials [26, 27]. In isothermal conditions the generated heat flows away, therefore little temperature rise is observed whereas in adiabatic condition the temperature can rise significantly [27]. The self-heating property is influenced by the strain rate [26]. A Higher strain rate increases the deformation rate leading to the thermodynamic condition transitions from isothermal to adiabatic. In the high velocity impact at higher strain rate, the generated heat does not get enough time to conduct away from regions of localized plastic deformation within the material due to the short duration of impact events [28]. The contribution of the strain rate becomes significant when combined with small mass impact [20]. Published literature on the strain-rate effects on the impact response of composites based on polymers are very limited, although polymer and foam materials are sensitive to strain rate. It was reported that the experimental investigation of the effects of strain rate on low velocity impact of sandwich composites have not yet been reported which could be due to two reasons- 1. The lower strain rate in low velocity impact testing as the used impact velocities are low, or 2. Larger impact mass since the mass of the target (sample mass) is smaller than that of the impactor dart [20]. It has been also found from previous investigations [29, 30] that friction

between the striker and the polymer sample is very important and can affect the location of the deformation and the impact strength recorded. Therefore, friction between the striker and the polymer sample must be taken into account especially for numerical analysis to predict and simulate the impact behaviour of polymers [31]. Duan et al. [31] used the friction co-efficient value μ =0.3 and μ =0 using the finite-sliding contact model in ABAQUS/Explicit package in order to simulate impact events with and without considering the friction between the impactor and polymer samples. It was observed that if the friction is not considered, simulated impact loads are significantly lower at larger displacements compared to experimental findings. O. Schang and N. Billon [29] used a lubricated impactor with oil in simulated and experimental lubricated impact tests as the friction coefficient was reported to be an important parameter quite difficult to measure. The similarities between experiment and simulation was found up to the maximum of the curve, but the model was not able to reproduce the decrease in strength.

The impact response of the rotationally moulded sandwich structure is crucial to the product performance and this needs to be accounted for the design, manufacture and maintenance of the sandwich structure. The failure mechanism and damage modes are complex as different damage modes may be seen at different layers of the sandwich structure. Casavola et al. [1] analysed the low velocity impact properties of rotationally moulded sandwich composites from 5 J to 70 J energy levels. In their investigation they used 3 mm thick outer and inner skin layers with a 38 mm thick core layer to create a 44 mm thick sandwich structure. The load over time, damage size and absorbed energy responses were analysed and compared to finite element simulation. They found a good agreement between the finite element model and experimental work up to 15 J energy levels and suggested as future work to build a damage model for higher energy levels.

The effects of related parameters such as skin and core thickness and their thickness ratios, impact velocity, impact dart diameter etc. on the impact properties and damage creation of the rotationally moulded sandwich structures have not been analysed yet in the literature, however. Therefore, to confirm the durability, reliability and safety of the rotationally moulded sandwich structures in various applications, further in-depth research on impact properties is necessary. In this work, the low velocity impact behaviour of rotationally moulded Polyethylene skin-foam-skin sandwich composites was tested experimentally using a drop weight impact tester to investigate the effects of varying skin and core layer thicknesses on impact response and damage creation at each layer of these sandwich structures. Rotationally moulded sandwich structures were manufactured at four common skin and core thickness combinations and tested under low velocity drop weight impact condition from 20 J to 100 J energy levels. The thickness of the sandwich structure skin and foam sections used here were based on the thicknesses typically used in marine leisure craft such as kayaks, canoes and small boats and automotive applications. In real life scenarios for these components, failure has been observed to be due to low velocity impact. Therefore, impact energy levels were selected for this study between 20 J to 100 J and the ratio of the impactor mass and effective plate mass ($\overline{m}$>8) was maintained according to the requirements of low velocity impact [19, 21-22]. Polyethylene (PE) was used for both the skin and foamed core layers in these samples tested as rotationally moulded PE is the most commonly used material in this industry, with higher resistance to fracture initiation and propagation compared to Polypropylene (PP) and other materials [32-33]. Following impact events, damage was identified at different layers of the sandwich structures using an optical microscope. Force-time, force-deflection and impact energy data were recorded using a load cell mounted on the impact dart and these were analysed to understand the skin and core layer thickness effects on low velocity impact response of rotationally moulded skin-foam-skin sandwich structures.

2. Experimental Work

2.1.Rotational moulding of sandwich structure samples

Rotationally moulded polyethylene sandwich samples were made using a Ferry Roto-speed Carousel type rotational moulding machine at Matrix Polymers Ltd. UK facilities. Material properties are listed in Table 1. PE was used for the skin layers while a blowing agent was blended with PE for the foam core layer.

Four different skin-core thickness combinations were produced and the respective shot-weight for each layer is presented in Table 2.

Mouldings were produced in a 300 mm steel cube mould. Polymer powder for the outer skin layer was introduced into the mould first, heated to 140 °C with rotation to form the outer layer. The mould was then taken out from the oven, the foamed core layer powder added, and heated to 130 °C. At 130°C the foam layer was melted without any expansion. After that the final polymer powder was added for the lower skin layer and processed in the oven up-to 170 °C. For the lower skin layer the higher 170°C temperature was used so that the blowing agent in the foam layer can be decomposed and expanded and also the lower layer can be formed. Finally, the mould was removed from the oven for cooling. Air cooling was applied with five minutes precooling to solidify the products before de-moulding was carried out. An example of the internal mould air temperature profile for manufacturing of sandwich-(1-4-1) type samples is given in Figure 3.

2.2.Low velocity impact test

Low velocity impact tests were carried out with an instrumented drop weight impact testing machine according to ASTM-D 3763 – 02 standards (Table 3) [34]. Impact sandwich samples

were cut from the 300 mm cube mould into 110×110 mm squares as per the testing standard and placed on the sample holder of the drop weight impact testing machine. The impact dart tip was a hemispherical indenter of 12 mm diameter attached to a 22.4 kN piezoelectric impact force sensor. The total falling mass of the impactor dart was 9.1 kg (included impactor and crosshead mass). A high-resolution oscilloscope (Picoscope IEPE 4242) was used to acquire the data generated from the load cell during the impact event. Impact force, time and deflection data were obtained for each test. The deflection term indicates the deflection of the upper (impacted) surface of the samples during contact between sample and impactor [35]. Here an anti-rebound system was not available and force-deflection curves represented only the primary impact of each impact event. Development of an anti-rebound system would be a very useful development for more detailed future work on this topic. Impact test energy levels were selected to maintain low velocity impact condition and 20, 30, 40, 50 and 70 J were used in this work for all sandwich samples. In-order to induce failure in the thicker samples tested, energy levels of 80 J and 100 J were also used for the sandwich-(2-4-2) and sandwich-(2-8-2) samples. Three specimens were tested at each energy level for all types of samples. In this work, effect of friction between the impactor and the sandwich sample on impact properties was neglected which will be considered in a separate study in future. Impacted samples were cut to examine the cross section of the impacted area. Impact damage was investigated at the upper and lower skin and at the cross section of impacted area using a digital optical microscope.

3. Results and discussion

3.1. Damage characterisation of the sandwich samples

Figure 4 to 6 show images of the upper and lower skin of the sandwich samples after low velocity impact tests from 20 J to 100 J impact energy levels. The damage modes of rotationally moulded sandwich samples were investigated from these sample images. At 20 J and 30 J

impact energy levels, no clear crack or fracture was observed in the upper skin (Figure 4) for all the samples tested. The only damage visible was the local plastic deformation and indentation depth in the upper skin.

The depth of the plastic deformation in the upper skin increases with increasing of the impact energy until fracture. For sandwich-(2-4-2) and sandwich-(2-8-2) samples, an increase of the depth of the plastic deformation without failure was observed up-to 70 J. Sandwich -(1-4-1) and sandwich-(1-8-1) also exhibited the similar result up-to 40 J and 50 J respectively before failure.

On the lower skin (Figure 5) a small protrusion was noticed following the impact tests which increased with the increase in impact energy. At 20 J, the protrusion was seen clearly in the sandwich-(1-4-1) samples with a crack forming on the lower skin at 30 J. Sandwich-(1-4-1) did not show fracture in the upper skin at 30 J and the impact dart was seen to penetrate the whole structure at 40 J. Penetration refers to the case where the dart fully passes through all layers of the sandwich samples [36]. From this observation it was concluded that the fracture starts in the lower skin first due to the deflection during the impact event. A similar observation was also found for sandwich-(1-8-1) samples. Sandwich-(1-8-1) exhibited cracks at 50 J in the lower skin whereas no crack was observed in the upper skin at this energy level. Penetration occurred for the sandwich-(1-8-1) samples at 70 J impact energy levels. On the lower skin of sandwich-(2-4-2), protrusion size was found to increase with energy level and at 70 J (Figure 5) impact energy some clear cracks were observed in the lower skin while full penetration occurred at 80 J (Figure 6). For sandwich-(2-8-2), the lower skin protrusion was clearly seen at 70 J (Figure 5) with some cracks were found at 80 J (Figure 6) impact energy. No crack was

observed at 70 or 80 J in the upper skin for sandwich-(2-8-2). Finally, 100 J (Figure 6) impact energy was enough to fully penetrate the sandwich-(2-8-2) samples.

Figure 7 shows the cross section of the sandwich samples after impact at 30 J and 70 J energy levels. From these images, it is seen that plastic deformation (indentation depth) in the upper skin, crushing in the core layer, and protrusion in the lower skin are the main deformation modes for the thicker sandwich-(2-4-2) and sandwich-(2-8-2) samples. No interfacial cracks or delamination at the skin/core interface was observed for any of the samples tested indicating that delamination is not a major concern under these kinds of impacts. The indentation of the upper skin and the protrusion at the lower skin were found to increase with increasing impact energy as expected. The reduction in thickness of the core layer also increased with increasing energy levels which reduced the local overall thickness of the sandwich samples. These deformations were permanent and would represent permanent visible damage in a real-world case.

Sandwich-(1-4-1) and sandwich-(1-8-1) also exhibited similar damage modes until their failure through penetration of the impact dart. For sandwich-(1-4-1) and sandwich-(1-8-1) samples, fracture was seen to start on the lower skin at 30 J and 50 J respectively, leading to full dart penetration at higher energy level. Sandwich-(2-8-2) showed the lowest amount of core crushing and thickness reduction among all the samples for the energy levels tested, this is likely due to the higher skin, core and overall thickness of this sample. Though sandwich-(1-8-1) samples are thicker compared to sandwich-(2-4-2) samples, they were found to have higher upper skin indentation depth, core crushing and protrusion in lower skin than that of in sandwich-(2-4-2) samples for the same energy levels (30 J and 70 J mentioned in Figure 7). This shows that the skin thickness plays a more crucial role in the impact damage resistance

than the core layer thickness. Sandwich-(1-8-1) showed better resistance compared to sandwich-(1-4-1) due to the thicker core region. Similar thicker core region effect was also found for sandwich-(2-4-2) and sandwich-(2-8-2) samples.

3.2.Impact test results of rotationally moulded skin-foam-skin sandwich structures

Force-deflection curves were recorded for 20 J, 30 J, 40 J, 50 J and 70 J energy levels respectively as shown in Figure 8 (A-E). From Figure 8 (A-E), it is seen that in general the impact force values were found to increase with the increase of both skin and core layer thickness. Deflection values were also found to decrease with the increase of core and skin layer thickness. Therefore, it can be said that the bending stiffness of rotationally moulded sandwich structure is proportional to both the foamed core and skin layer thickness. Sandwich-(2-8-2) exhibited the highest recorded force and lowest deflection value at every energy level among all the sandwich samples as expected due to its higher overall thickness and stiffness. Similarly, sandwich-(1-4-1) showed the lowest force value at each energy level as it is the thinnest sandwich structure tested. It also showed the greatest deflection at 20 J and 30 J before penetration at the 40 J energy level. The foamed core thickness of sandwich-(1-8-1) is twice that of the sandwich-(1-4-1) and due to this sandwich-(1-8-1) showed higher force and lower deflection compared to sandwich-(1-4-1). Sandwich-(2-4-2) and sandwich-(1-4-1) both have a 4-mm core thickness with 1 and 2 -mm skin thicknesses respectively. This 1-mm increase in the skin thickness of sandwich-(2-4-2) was seen to result in higher force and lower deflection than for sandwich-(1-4-1). It also showed higher stiffness (higher force and lower deflection) than the 8-mm core sandwich-(1-8-1), despite having a lower overall thickness (10mm vs. 8mm). From these results it can be said that the skin thickness has a greater contribution to the impact resistance of this sandwich structure under low velocity impact than the foamed core

thickness. Similar observations were also found when comparisons were made among the sandwich-(2-8-2), sandwich-(2-4-2) and sandwich-(1-8-1) samples.

The loading and unloading portion of the force – deflection curves at Figure 8 (A-E) provide information on damage mechanisms. The loading portion of the curves was almost the same for all the samples while the unloading portion showed some differences. At 20 J impact energy levels (Figure 8-A) only one peak was observed for all the samples which indicates that 20 J energy was not enough to create fracture or significant penetration of the samples. Similarly, at 30 J and 40 J energy levels (Figure 8- B, C) only one peak was also observed for all samples except sandwich-(1-4-1). Sandwich-(1-4-1) showed a sudden decrease in the force-deflection curve at 30 J impact energy indicating that fracture at the lower skin had occurred. Two clear peaks and penetration of the dart are seen at the 40 J energy level (Figure 8-C). The first peak indicates failure of the lower skin layer as the fracture initiates and the second peak indicates fracture of the upper skin layer. No extra peak was observed for the foam layer indicating that this provides little resistance to impact beyond adding stiffness to the sample. At this energy level, the impactor was not observed to return from the samples due to sample penetration and due to this the unloading portion of the sandwich-(1-4-1) samples was not found to return to the X-axis. Sandwich-(1-8-1) showed fracture in its lower skin layer when tested at 50 J (Figure 8-D) and this was also seen as a sudden drop in the force-deflection curve. Full dart penetration occurred in sandwich-(1-8-1) at 70 J (Figure 8-E) impact energy. Sandwich-(1-4-1) showed the penetration at both energy levels (50 J and 70 J) as it is expected. Sandwich-(2-4-2) and sandwich-(2-8-2) samples exhibited only one peak during the 50 J and 70 J energy level tests indicating that no fracture or penetration of the lower surface had occurred, and this was also seen when inspecting the sample was done.

Figure 9 (A-C) shows the maximum impact force-impact energy curves of sandwich samples for all the thicknesses tested. It is clear that the maximum impact force increases with increasing skin and core thickness, and that skin thickness contributes more to the increase of maximum impact force than core thickness. The maximum impact force of sandwich-(2-4-2) and sandwich-(2-8-2) increased very rapidly at every energy level as they did not get any fracture or penetration at these energy levels. For sandwich-(1-4-1) the maximum impact force increased quickly up-to 40 J impact energy level when failure occurred. After that it increased slowly and from 50 J no significant change was observed, therefore this indicates the maximum energy this sample can absorb before dart penetration. A similar trend was also noticed for sandwich-(1-8-1) samples where initially the maximum force increased rapidly up-to 50 J before it slowed down when fracture and penetration occurred above this energy.

Contact time-impact energy graphs for the samples tested are shown in Figure 9- B. From this figure it is found that in general contact time decreases with the increase in skin and core layer thickness, and that skin layer thickness is contributing more to the reduction of the contact time during impact than core layer thickness. Sandwich-(1-4-1) showed the highest contact time at 20 and 30 J energy levels. From 40 J it decreased suddenly because of the penetration and this value remained consistent for other energy levels. Sandwich-(1-8-1) exhibited lower contact time than sandwich-(1-4-1), though it showed higher contact time compared to sandwich-(2-4-2). Similar trend was also noticed between sandwich-(1-8-1) and sandwich (2-8-2). Contact time was also found to decrease from 50 J for sandwich-(1-8-1) samples because of the observed penetration and fracture in the structure. The lowest contact time was noticed for sandwich-(2-8-2) samples among all the samples at each energy level as expected because of its highest thickness.

The maximum deflection-impact energy curves in Figure 9-C show the expected behaviour. Deflection during the impact event at each energy level decreases with the increase in skin and core layer thickness because of the increase in bending stiffness of the sandwich samples tested here. In this analysis increasing skin layer thickness is also found to be more responsible for the decrease in deflection compared to the core layer thickness as we found for the maximum contact force and contact time analysis. Sandwich – (1-4-1) showed the highest deflection at 20 J and 30 J of all the samples tested with the deflection reducing dramatically due to upper skin penetration after 30 J. The Sandwich-(1-8-1) samples showed lower deflection than the sandwich-(1-4-1) samples, and from 50 J the deflection was observed to decrease suddenly due to the fracture and penetration of the samples. Lower deflection was found for sandwich-(2-4-2) compared to sandwich-(1-8-1). The lowest deflection was noticed for sandwich-(2-8-2) because of its highest thickness.

In this work, 80 J and 100 J energy levels were also used for sandwich-(2-4-2) and sandwich-(2-8-2) samples to investigate their penetration energy level as these samples were found to not fail at lower impact energies. It was found that sandwich-(2-4-2) was penetrated at 80 J and for sandwich-(2-8-2) it occurred at 100 J energy level which are also presented here in Figure 6 of section 3.1.

3.3.Discussion

Cross sections of the impacted samples, upper and lower skins showed that the fracture starts from the lower skin of the sandwich samples, and this was also seen in the drop of the force-deflection curves. Damage analysis identified the plastic deformation in the upper skin, protrusion in the lower skin and crushing in the core as the main damage modes. Delamination at the skin/core interface was not observed here for any test.

From the above results, it was found that the maximum impact force increased while deflection and contact time decreased with the increase in core and skin layer thickness at each impact energy level. Therefore, it was concluded that the resistance to impact force increases with the increase in both skin and core layer thickness for these rotationally moulded sandwich samples. Raju et al. [24] also observed the higher peak force and reduced impact duration with an increase in the skin thickness of honeycomb core and plain weave carbon fabric/epoxy prepreg skin sandwich composites. A thicker core also exhibited higher impact force and resistance to impact force in previous work [37]. Peak impact force, contact time and deflection analysis proved that an increase in skin layer thickness offers better resistance to impact force compared to an increase in core layer thickness. From the comparison of all the thicknesses tested in this work, it was observed that increasing the skin thickness twice enhances the fracture initiation or penetration energy level more than 100% while for the foam core less resistances are found. In this investigation, it was noticed that during the impact event the impactor hits the upper skin, transfers energy to the sandwich sample, and creates the indentation depth, core crushing and protrusion in the upper skin, core layer and lower skin respectively. At higher energy levels, indentation depth and protrusion in the upper and lower skin increases respectively until failure of the lower skin occurs. Similarly, the core layer thickness is reduced with higher energy levels. As the energy level approaches that needed to cause failure in the sample, the lower skin fractures, and the crack then continues to grow through the crushed and consolidated core layer until it reaches the upper skin, before finally the upper skin cracks and fails as the impact dart penetrates. A thicker core layer is seen to accommodate more crushing and consolidation than a thinner core layer and this helps to improve impact resistance by reducing the deformation in lower skin and penetration of whole structure as well. An increase in upper and lower skin thickness enhances higher bending stiffness, better resistance to impact force and an accommodation for more core crushing and consolidation compared to an increase only in core

layer thickness that ultimately prevents the penetration at higher impact energy level for the thicker skin sandwich samples.

In these tests each impact was seen to result in plastic deformation on the upper skin, this was easily identified visually and considered not problematic to find out as like as the detection of barely visible impact damage in sandwich structures [38]. Similarly, the initial failure of the sandwich was seen to occur on the lower skin in all cases and this can be used to assess damage on the component when only the lower or inner skin is visible such as boat hull. Moreover, no catastrophic or localised failure was observed in the skin or core layer which is also advantageous to avoid any sudden failure incident in service life of this rotationally moulded sandwich components.

4. Conclusions

Impact response

Resistance to impact force of the rotationally moulded sandwich samples increased with the increase of both skin and core layer thickness as the maximum impact force was found to increase, while deflection and contact time were observed to reduce at each energy level for thicker skin/core combinations. The results indicate that increasing skin layer thickness was more responsible for enhancing the impact resistance of the sandwich samples than increasing core layer thickness. It was noticed that doubling the skin thickness enhances the fracture initiation or penetration energy level more than hundred percent while for the foam core less resistances are found.

Damage

Indentation in the upper skin, protrusion in the lower skin and crushing and consolidation in the core layer were each identified as the damage modes under impact for the samples. Each of these effects was seen to increase with increasing energy levels for all samples tested. No

delamination at the core/skin interface was observed. Fracture was seen to start from the lower skin, continued to grow in the core layer, before finally reaching the upper skin when penetration occurs. A thicker skin layer increased more impact resistance compared to thicker core layer by providing a better accommodation for more crushing and consolidation in core layer and enhancement of bending capability that ultimately prevented fracture initiation or penetration at higher impact energy level. No sudden or catastrophic failure was observed, damages in core and skin layers were identified as visible impact damages which were easy to find out.

Design Implications

The findings of this work provide a better understanding about the low velocity impact behaviour of these tested sandwich structures. It is hoped this investigation would be helpful to create design guidelines particularly thickness of structures, likely impact energies facing in real life scenario and impact damage inspections of these sandwich structure in various applications such as marine leisure crafts or automotive sectors.

References

[1] C. Casavola, V. Moramarco, and C. Pappalettere, *Fatigue & Fracture of Engineering Materials & Structures,* **37**, 1377 (2014).

[2] A. Boccaccio, C. Casavola , L. Lamberti, and C. Pappalettere, *Materials*, **6**, 4545 (2013).

[3] R. Pop-Iliev, K.H. Lee, and C.B. Park, *Journal of Cellular Plastics*, **42**, 139 (2006).

[4] M.C. Cramez, M.J. Oliveira , and R.J. Crawford, *Polym. Degrad. and Stab.*, **75** , 321 (2002).

[5] R.J. Crawfoard and M.P. Kearns, *Introduction to the Rotational Moulding Process*, *in Practical Guide to Rotary Moulding*, Shrewsbury (2003).

[6] R.J. Crawfoard, *Journal of Materials Processing Technology*, **56**, 263 (1996).

[7] R.C. Vázquez-Fletes, L.C. Rosales-Rivera, F.J. Moscoso-Sánchez, E. Mendizábal, P. Ortega-Gudiño, and R. González-Núñez, *Polymer Engineering & Science*, **56**, 278 (2016).

[8] S. Banerjee, W. Yan and D. Bhattacharyya, *Polymer Engineering & Science*, **48**, 2188 (2008).

[9] A. A. Aissa, C. Duchesne and D. Rodrigue, *Polymer Engineering & Science*, **52**, 953 (2012).

[10] M. Asgarpour, F. Bakir, S. Khelladi, A. Khavandi and A. Tcharkhtchi, *Polymer Engineering & Science*, **52**, 2033 (2012).

[11] R.H. López-Bañuelos, F.J. Moscoso, P. Ortega-Gudiño, E. Mendizabal, D. Rodrigue and R. González-Núñez, *Polymer Engineering & Science*, **52**, 2489 (2012).

[12] E. Archer , E. Harkin-Jones , M.P. Kearns, A.-M. Fatnes, *Journal of Cellular Plastics*, **43**, 491 (2007).

[13] R. González-Núñez, F. J. Moscoso-Sánchez, J. Aguilar , R. G. López-GonzálezNúñez, J. R. Robledo-Ortíz and D. Rodrigue, *Polymer Engineering & Science*, **58**, 235 (2018).

[14] A. Marcilla , J.C. García-Quesada, R. Ruiz-Femenia and M. I. Beltran, *Polymer Engineering & Science*, **47**, 1804 (2007).

[15] G. Liu, C. B. Park and J. A. Lefas, *Polymer Engineering & Science*, **38**, 1997 (1998).

[16] K. Duffy, U.S. Patent, US4952350 A (1990).

[17] L.S. Sutherland and C.G. Soares. *Composites Part B : Engineering*, **43**, 1459 (2012).

[18] S. Abrate, *Applied Mechanics Reviews*, **50**, 69 (1997).

[19] S. Abrate, *Impact on composite structures,* Cambridge (2005).

[20] G.B. Chai, and S. Zhu, *Proceedings of the Institution of Mechanical Engineers, Part L: Journal of Materials Design and Applications,* **225**, 207 (2011).

[21] W.J. Cantwell, and J. Morton, *Composites*, **22**, 347 (1991).

[22] R. Olsson, *Composites Part A: Applied Science and Manufacturing,* **31**, 879 (2000).

[23] M.L. Bernard and P.A. Lagace, *Journal of Reinforced Plastics and Composites,* **8**, 432 (1989).

[24] K.S. Raju, B.L. Smith, J.S. Tomblin, K.H. Liew and J.C. Guarddon, *Journal of Composite Materials,* **42**, 385 (2008).

[25] G. Zhou, M. Hill and N. Hookham, *Journal of Sandwich Structures & Materials,* **9**, 309 (2007).

[26] F. Shen, G. Kang, Y.C. Lam, Y. Liu and K. Zhou, *International Journal of Plasticity,* **121**, 227 (2019).

[27] D. Rittel, *Mechanics of Materials,* **31**, 131 (1999).

[28] C. Sorini, A. Chattopadhyay and R.K. Goldberg, *Composite Structures,* **215**, 377 (2019).

[29] O. Schang and N. Billon, *Polymer Engineering & Science*, **36**, 541 (1996).

[30] R. P. Nimmer, *Polymer Engineering & Science*, **23**, 155 (1983).

[31] Y. Duan, A. Saigal and R. Greif, *Polymer Engineering & Science*, **43**, 112 (2003).

[32] A. Saifullah, B. Thomas , R. Cripps, K. Tabeshfar, L. Wang and C. Muryn, *Polymer Engineering & Science,* **58**, 63 (2018).

[33] A. Saifullah, B. Thomas , K. Tabeshfar K, and R. Cripps, *Annual Technical Conference-ANTEC, Conference Proceedings*, 1686 (2016).

[34] ASTM-D3763-02, *Standard Test Method for High Speed Puncture Properties of Plastics Using Load and Displacement Sensors*.

[35] C. Atas and U. Potogˇlu, *Journal of Sandwich Structures and Materials,* **18**, 215 (2016).

[36] O. Ozdemir, R. Karakuzu and A.K J. Al-Shamary, *Journal of Composite Materials,* **49**, 1315 (2015).

[37] N. Sawal, and M.A. Hazizan, *Key Engineering Materials: Trans Tech Publ*, 461 (2011).

[38] P. Compston , M. Styles , and S. Kalyanasundaram, *Journal of Sandwich Structures and Materials*, **8**, 365 (2006).

Table 1: Material properties used in rotationally moulded sandwich composites*.

Materials Grade	**Material Type**	**Layer**	**MFI (g/10 mins)**	**Density (g/cm^3)**	**Yield Stress (MPa)**
Revolve M-601	PE	Skin	3.50	0.949	21.5
M-56	PE	Core	3	0.310	N/A

*Data provided by the materials provider (Matrix Polymers, UK).

Table 2: Shot weights (polymer powder quantity) used in making rotationally moulded sandwich composites.

Sandwich Type	**Thickness Combination (Skin + Core + Skin) (mm)**	**Shot weights (g) (Skin + Core +Skin)**
Sandwich-(1-4-1)	1+4+1	450+300+400
Sandwich-(1-8-1)	1+8+1	450+600+400

Sandwich-(2-4-2)	2+4+2	850+300+800
Sandwich-(2-8-2)	2+8+2	850+600+800

Table 3**:** Low velocity impact test of rotationally moulded skin-foam-skin sandwich samples.

Energy Level (J)	**Sandwich-(1-4-1)**	**Sandwich-(1-8-1)**	**Sandwich-(2-4-2)**	**Sandwich-(2-8-2)**	**Sample Dimensions mm× mm**	**Diameter of Indenter**	**Mass of Falling Dart**	**No. of Sample Tested**
20	X	X	X	X				
30	X	X	X	X				
40	X	X	X	X	110×110	12 mm	9.1kg	3

50	X	X	X	X				(each energy level)
70	X	X	X	X				
80	-	-	X	X				
100	-	-	X	X				

X= tested under above mentioned impact energy level, - = Not tested under above mentioned impact energy level.

Figure Legends

Figure 1 Rotationally moulded skin-foam-skin sandwich structure.

Figure 2 Rotational moulding process [7].

Figure 3 Internal mould air temperature profile for manufacturing of sandwich-(1-4-1) type samples. A = mould was opened for adding the foam layer, B = mould was opened for adding the lower skin layer, C= mould was removed from the oven to the cooling unit.

Figure 4 Damage of upper skin of the sandwich samples.

Figure 5 Damage of lower skin of the sandwich samples.

Figure 6 Damage of upper and lower skin of sandwich-(2-4-2) and sandwich-(2-8-2) at 80 J and 100 J.

Figure 7 Cross section of the impacted sandwich samples at 30 J and 70 J for all thicknesses.

Figure 8 Impact force-deflection curves of sandwich samples for various thicknesses at - (A) 20 J, (B) 30 J, (C) 40 J, (D) 50 J, (E) 70 J.

Figure 9 (A) Maximum force- impact energy, (B) Contact time- impact energy, (C) Maximum deflection-impact energy graphs for all samples.

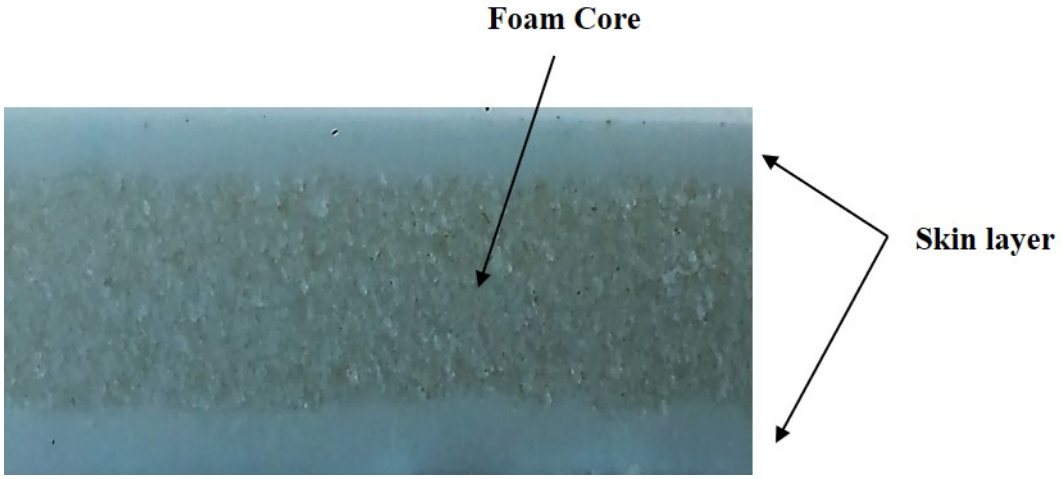

Figure 10 Rotationally moulded skin-foam-skin sandwich structure.

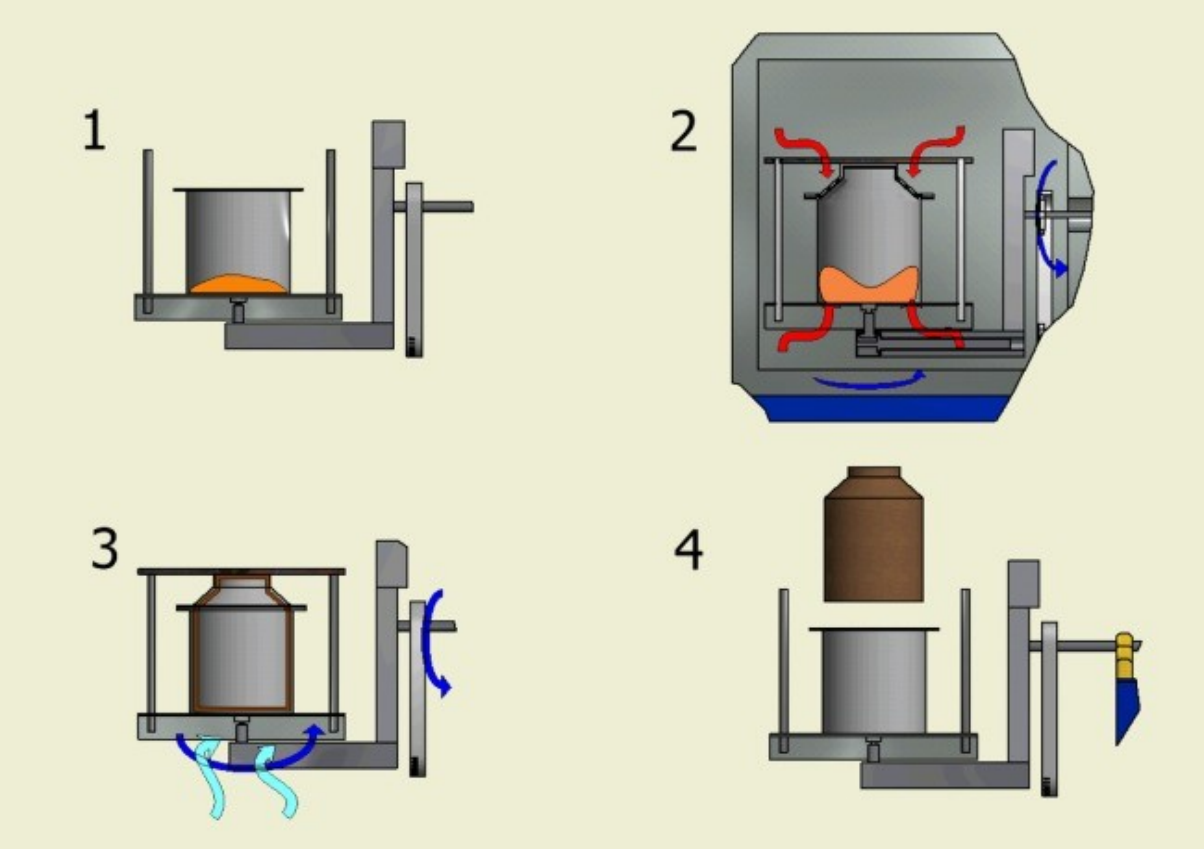

Figure 11 Rotational moulding process [7].

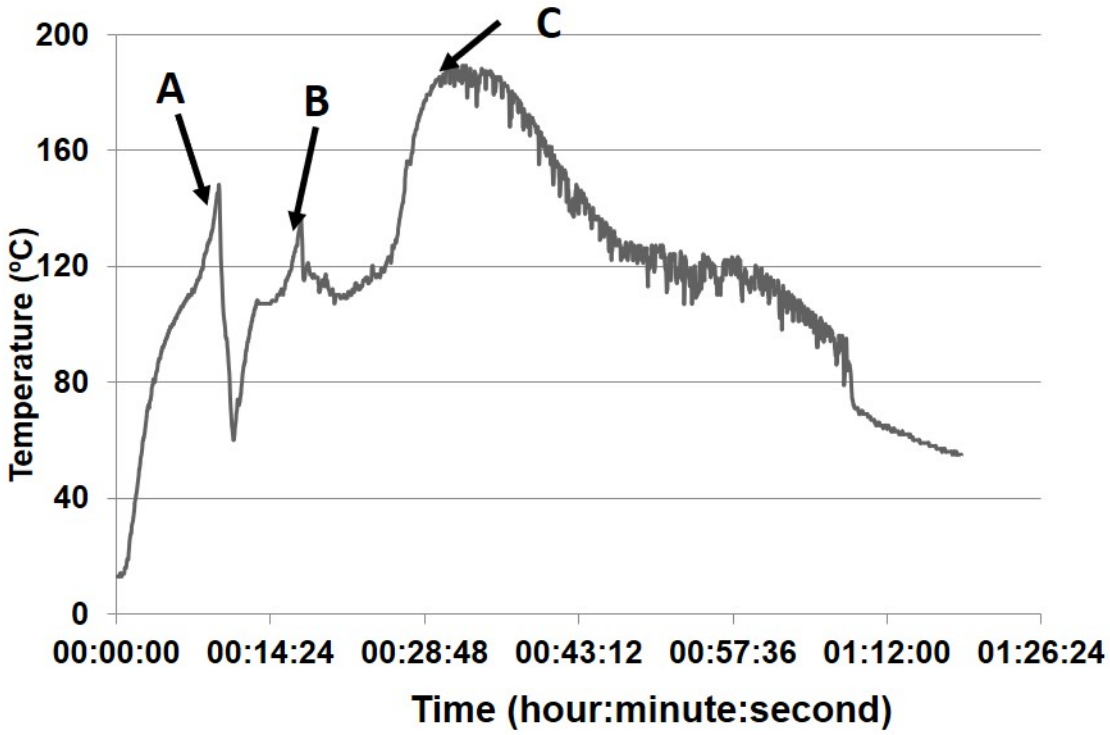

Figure 12 Internal mould air temperature profile for manufacturing of sandwich-(1-4-1) type samples. A = mould was opened for adding the foam layer, B = mould was opened for adding the lower skin layer, C= mould was removed from the oven to the cooling unit.

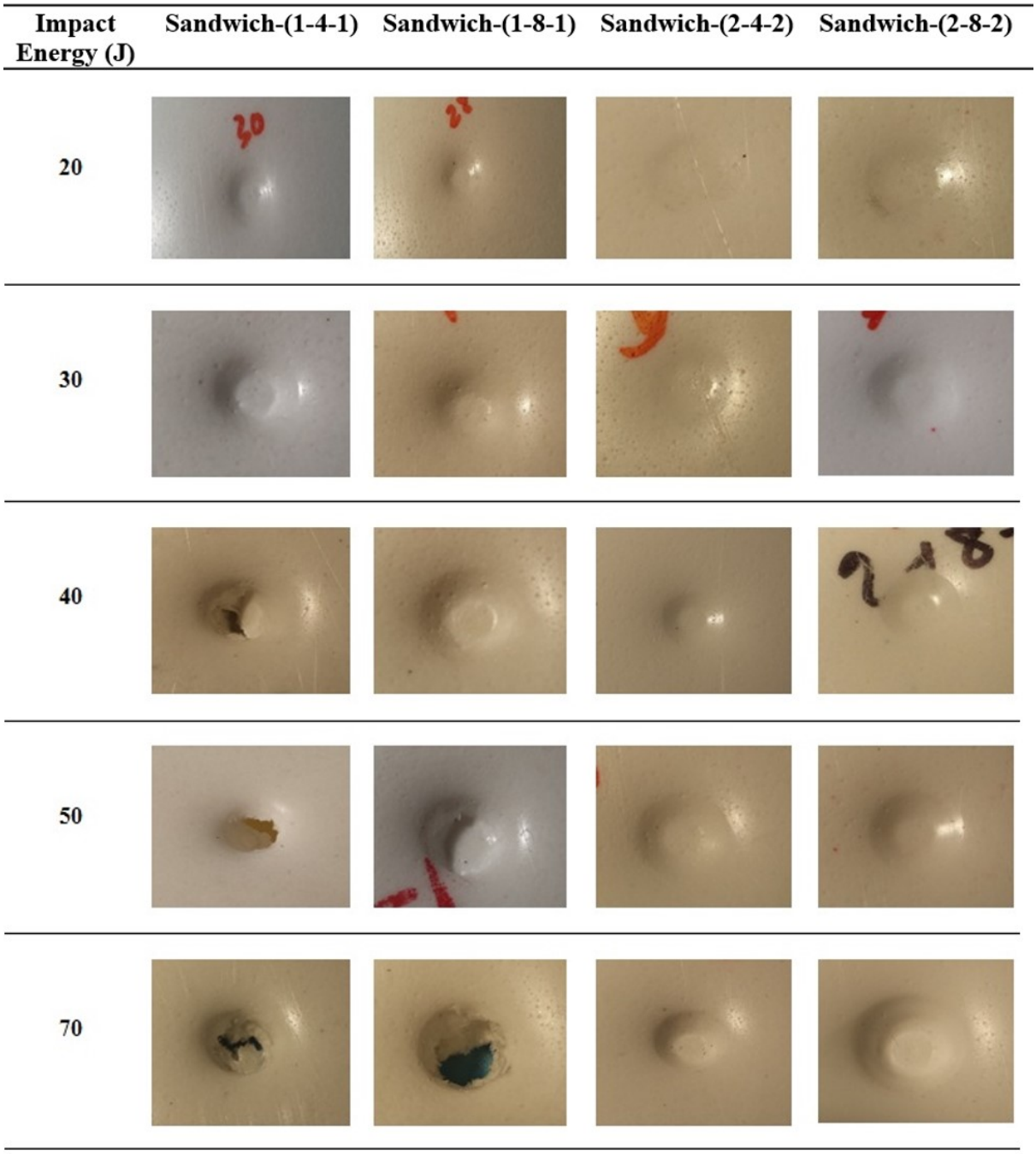

Figure 13 Damage of upper skin of the sandwich samples.

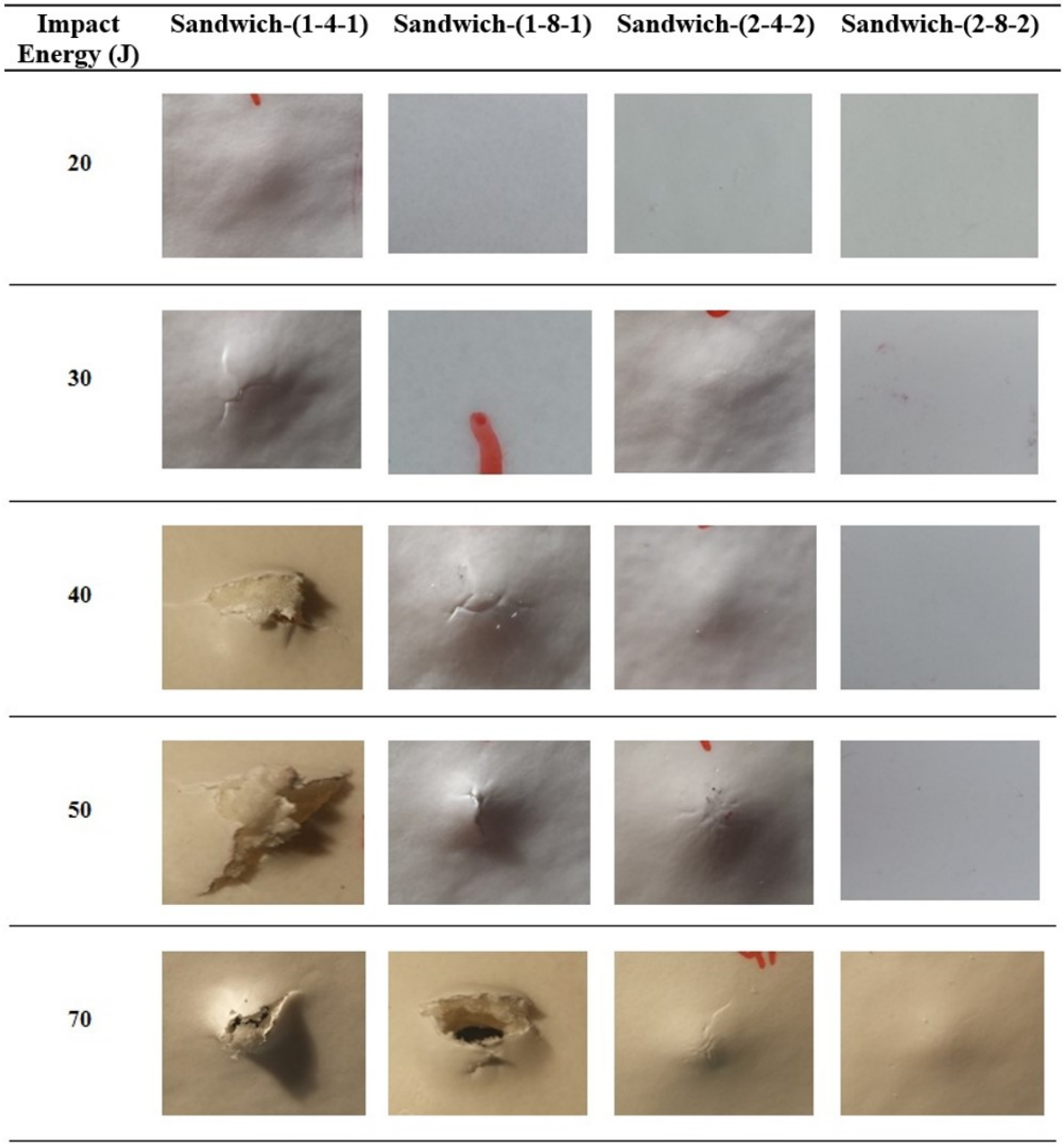

Figure 14 Damage of lower skin of the sandwich samples.

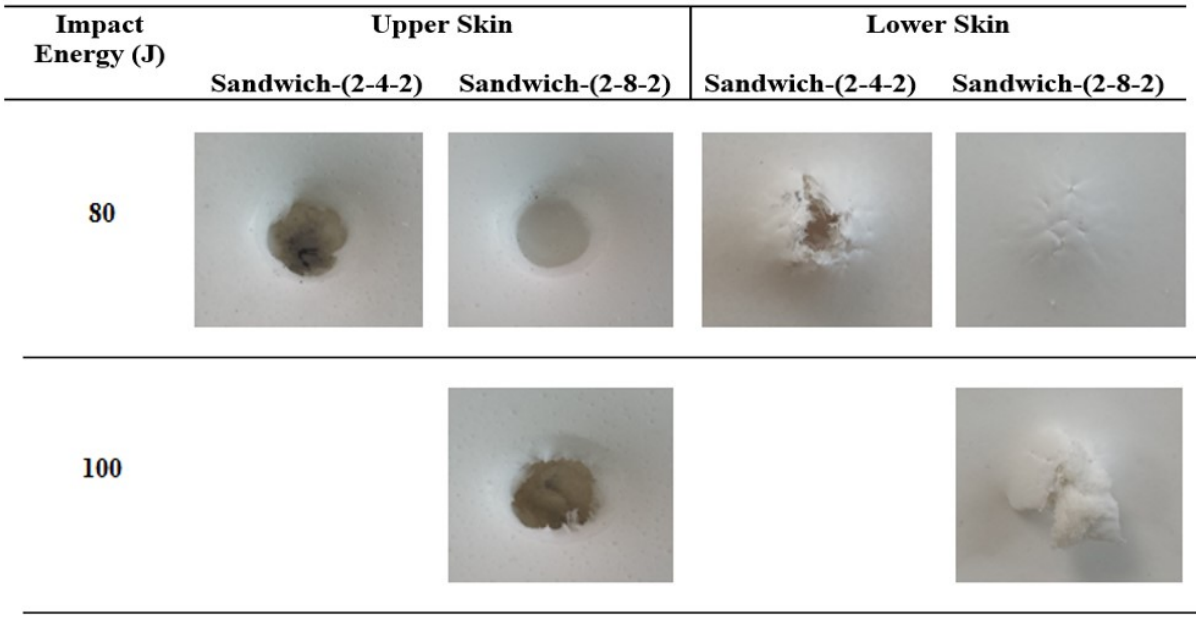

Figure 15 Damage of upper and lower skin of sandwich-(2-4-2) and sandwich-(2-8-2) at 80 J and 100 J

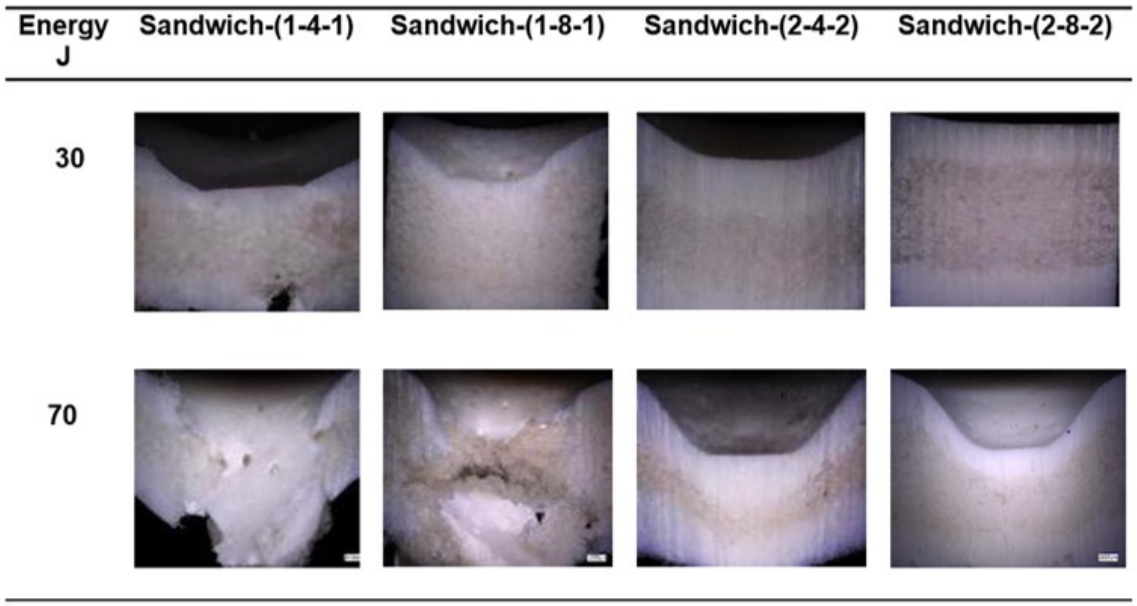

Figure 16 Cross section of the impacted sandwich samples at 30 J and 70 J for all thicknesses.

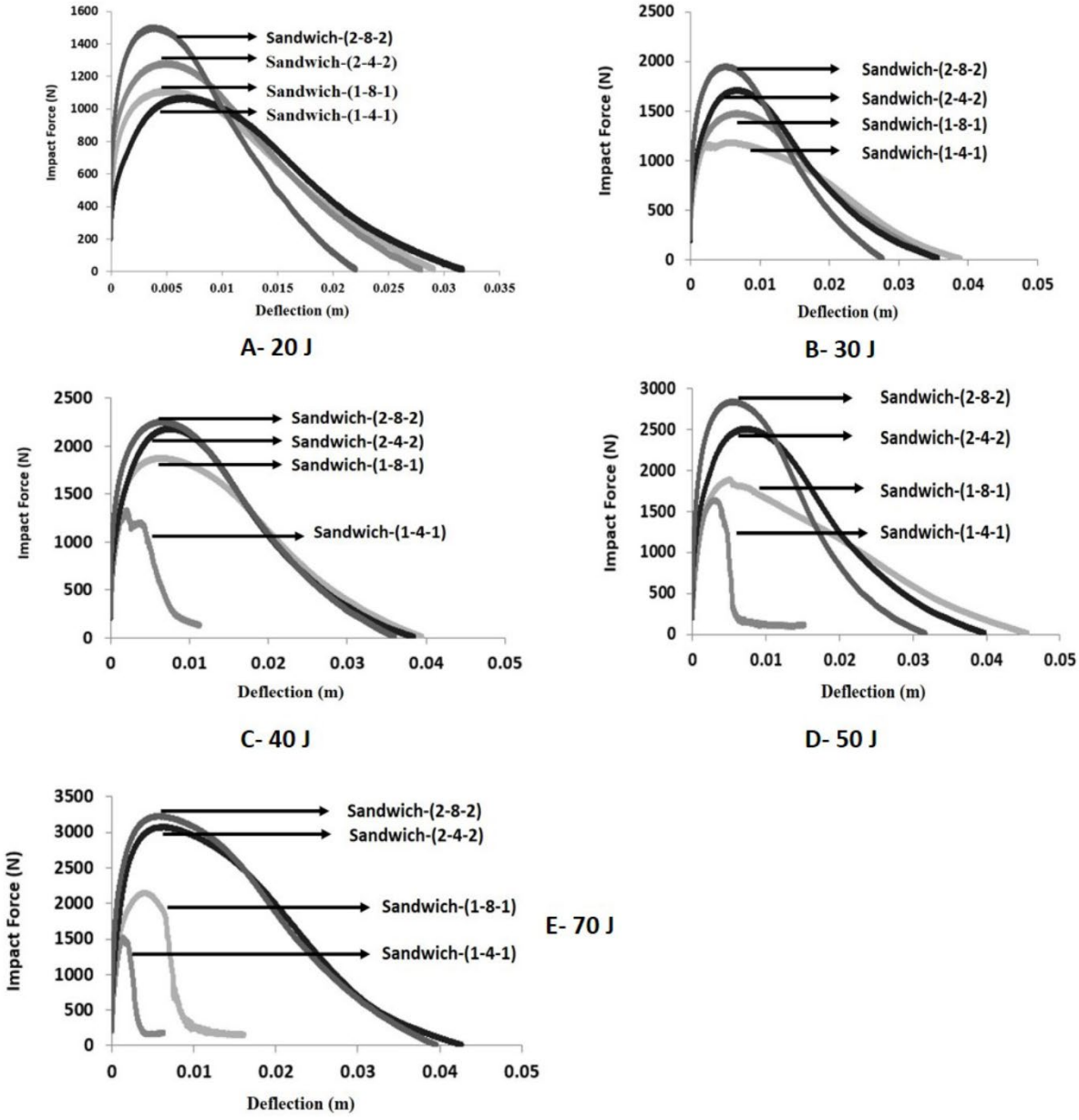

Figure 17 Impact force-deflection curves of sandwich samples for various thicknesses at - (A) 20 J, (B) 30 J, (C) 40 J, (D) 50 J, (E) 70 J.

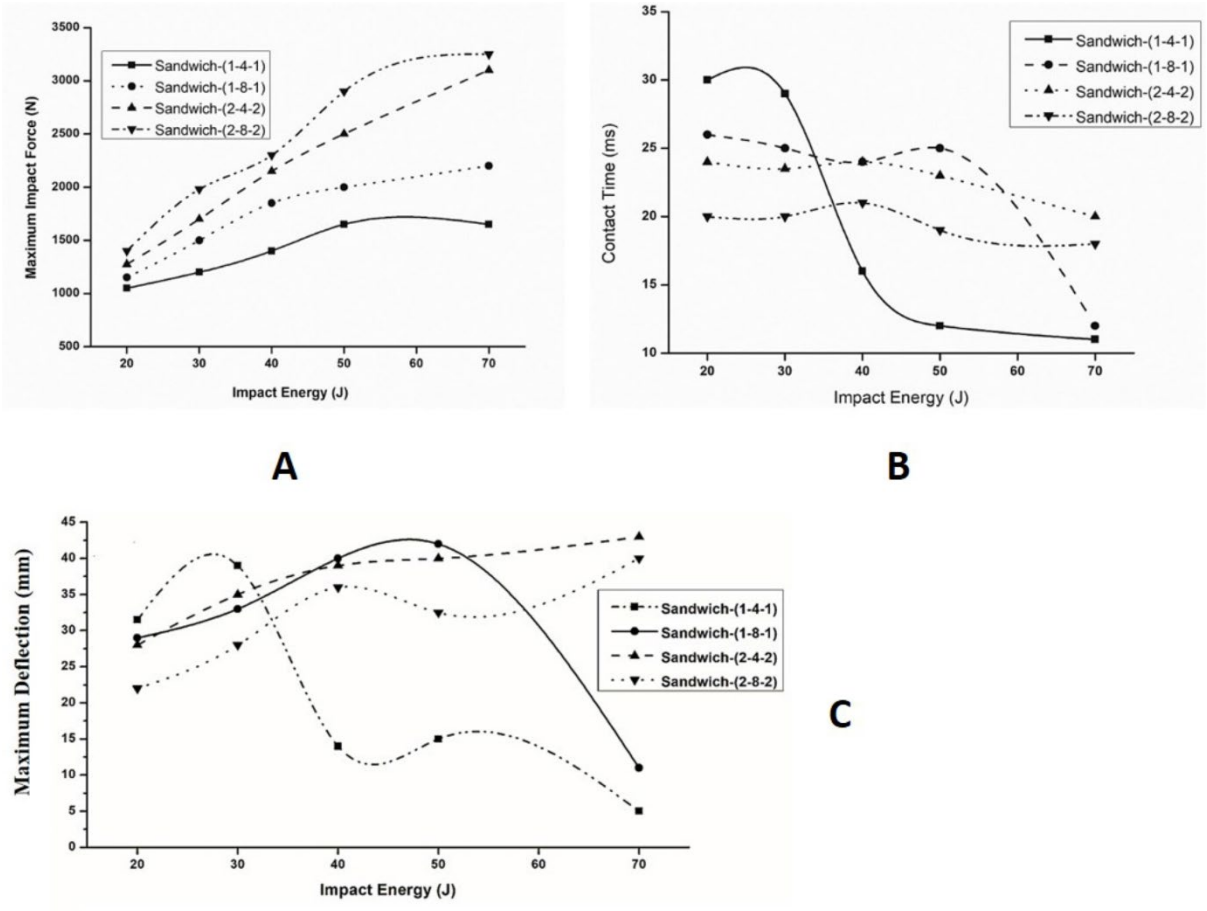

Figure 18 (A) Maximum force- impact energy, (B) Contact time- impact energy, (C) Maximum deflection-impact energy graphs for all samples.